***BRAF* mutation and *CDKN2A* deletion define a clinically distinct subgroup of childhood secondary high-grade glioma**

Mistry, *et al*.

Supplemental Materials and Methods

Patient Characteristics and Tumor Samples

26 patients were identified for PLGG transformation. 20 patients had matched consecutive low and high grade histological diagnoses; 3 patients had low grade histological diagnosis, followed by at least one year of stable disease, and then high grade diagnosis as determined by radiologic evidence (Fig S1); 3 patients had radiologic evidence of low grade disease, at least 1 year stable disease, followed by histological high grade diagnosis (Fig. S1). All PLGG and corresponding sHGG were re-reviewed by the study pathologist (C.E.H.). Tumor tissue for genetic and molecular analyses was available from 18 low-grade and 18 high-grade tumors, from a total of 24 patients. Two patients had no tissue available. Genomic DNA was extracted from formalin-fixed paraffin embedded tumor tissue utilizing the RecoverAll Total Nucleic Acid Isolation Kit (AM 1975) according to instructions from the manufacturer (Life Technologies). Genomic DNA was also extracted from snap frozen tumor tissue and peripheral blood utilizing the Qiagen DNeasy Blood and Tissue kit according to instructions from the manufacturer (Qiagen)[1].

Whole-Exome Sequencing (WES) Analysis

WES was performed on a discovery cohort of 7 sHGG, 2 patient matched PLGG and 5 patient matched germline samples at The Center for Applied Genomics (TCAG) at the Hospital

for Sick Children (7 patients total). No germ-line tissue was available for 1 patient (#19) so the patient's low grade tumor was used as the control to call somatic mutations in the high grade counterpart. Another patient (#7) developed myeloid dysplastic syndrome so a matching fibroblast cell line from the same patient was used as a control to call somatic mutations in the sHGG (total n=7 sHGG with matching control tissue to call somatic variants).

3-6μg of genomic DNA was submitted for target capture with the Illumina TruSeq exome enrichment kit (Illumina) and 100 bp paired-end sequencing reads on the Illumina 2000 HiSeq platform (Illumina) with bioinformatics processing and variant annotations as previously described at TCAG (The Hospital for Sick Children). Sequence were aligned to the reference human genome hg19 with BWA 0.5.9; Mark Duplicates (picard-tools-1.79) was used to remove any duplicate paired-end reads and the subsequent duplicate-free alignments were refined using Genome Analysis TK (GATK) 1.1-28; base quality recalibration was also performed using (GATK) 1.1-28. Somatic variant calling was performed using MuTect v1.1.4 with cosmic v63 (Broad Institute) [2]. Mutation totals for sHGG were calculated by including only those SNVs identified in the tumor and not in the matching germline tissue and mutations predicted to be potentially deleterious by changing the coding of a protein (i.e., nonsynonymous coding, stop codon lost, and stop codon gain mutations). Non-silent SNV totals from 65 pediatric primary HGG were taken from a previously published available exome sequencing data to compare against sHGGs [3].

Sanger Sequencing Analysis

We investigated candidate somatic point mutations and glioma hotspots in a validation cohort of patients for which genomic DNA was available. 50 ng of genomic DNA from patients

was used to amplify exon 15 of *BRAF*, exon 4 of *IDH1* and exon 2 of *H3F3A* with the use of a polymerase-chain reaction (PCR) assay as previously described. 5µl of PCR product was treated with 2µl Exo-SAP-IT (Affymetrix) and sequenced using the Sanger method as previously described [4-6]. Sequencing chromatograms were manually curated for hotspot mutation detection.

Percentage of mutant *BRAF* alleles by castPCR

The *BRAF* mutation status was determined with commercially available TaqMan Mutation Detection Assay (Applied Biosystems). Competitive allele-specific TaqMan PCR (castPCR) using the BRAF_476_mu probe for the detection of the *BRAF* c.1799T>A mutation were run in triplicates on an Applied Biosystems 7900HT Fast Real-Time PCR System. The mutant allele frequency was determined by comparing the cycle threshold (C_t) values of the wild-type and mutant allele assays (ΔC_t) in reference to the control samples using Mutation Detector software 2.0. The percentage of mutant *BRAF* alleles was calculated as $\%=1/(2^{\Delta Ct}) \times 100$ [7]. All *BRAF* mutant positive samples by Sanger were validated by castPCR.

Genotyping Assay for *hTERT* Promoter Mutations:

Two primers (forward primer, 5′- CAG CGC TGC CTG AAA CTC -3′; reverse primer, 5′- GTC CTG CCC CTT CAC CTT C -3′) were designed to amplify a 163-bp product encompassing C228T and C250T hotspot mutations in the *TERT* promoter – corresponding to the positions 124bp and 146bp, respectively, upstream of ATG start site. Two fluorogenic LNA probes were designed with different fluorescent dyes to allow single-tube genotyping. One probe was targeted to WT sequence (*TERT* WT, 5′-5HEX-CCC CTC CCG G -3IABkFQ-3′), and one was targeted to either of the two mutations (*TERT* mut, 5′-56FAM-CCC CTT CCG G -3IABkFQ). Primer and probe design was performed by using Primer Express software, version

3.0 (Applied Biosystems, Burlington, ON, Canada), and sequence homogeneity was confirmed by comparison to all available sequences on the GenBank database by using BLAST (http://www.ncbi.nlm.nih.gov/BLAST/). Primers have been checked for hairpins, homo- and hetero-dimers. Primers and probes were obtained from Integrated DNA Technologies (Coralville, Iowa, USA).

Real-time PCR was performed in 25-µl reaction mixtures containing 12.5 µl of TaqMan Universal Master Mix II with UNG (Applied Biosystems), 900 nM concentrations of each primer, 250 nM *TERT* WT probe, 250 nM *TERT* MUT probe, and 1 µl (25 ng) of sample DNA. Thermocycling was performed on the StepOnePlus (Applied Biosystems) and consisted of 2 min at 50°C, 10 min at 95°C, and 40 cycles of 95°C for 15 s and 60°C for 1 min.

Analysis was performed by using StepOne Software, version 2.1. Samples were considered mutant if they had CT values of ≤39 cycles. Each sample was verified visually by examining the PCR curves generated to eliminate false positives due to aberrant light emission. End-point allelic discrimination genotyping was performed by visually inspecting a plot of the fluorescence from the WT probe versus the MUT probe generated from the post-PCR fluorescence read [8].

Raw Data Analysis – Comparative Genomic Hybridization (CGH) array

Genomic copy number alterations (CNA) of tumor samples from the same discovery cohort used for WES (7sHGG and 2 patient matched PLGG) were profiled using the genome wide CytoSure ISCA array (ISCA v2 4X180K) by Agilent. Feature extraction files were analyzed for CNAs using Partek Genomics Suite (PGS) version 6.6 (Partek Incorporated, St Louis, MO) as previously described[9]. Briefly, LogRatio values were imported into PGS and

normalized using quantile normalization. Copy number data was generated from Log_2 ratio values. The genomic segmentation and HMM tools available from PGS were used to determine regions of gains and losses with copy number >2.5 considered a gain and <1.5 considered as a loss. Homozygous deletions were considered below 0.5. Only genes with CNAs reported by both algorithms were included in the results. CNA genome rates per sample were reported using segmentation analysis. The deletion of *CDKN2A* was the only CNA validated using real-time qPCR.

Copy number assays (real-time qPCR) for *CDKN2A* gene deletions

The copy number for *CDKN2A* was determined using 2 commercially available and pre-designed TaqMan Copy Number Assays according to the manufacturer's instructions (Applied Biosystems). The primer IDs used for *CDKN2A* were Hs03714372_cn and Hs00965010_cn. The human RNase P H1 RNA gene was used as an internal reference copy number. Real-time quantitative PCR (in quadruplicates) was performed in a total volume of 20µl in each well, containing 10µl of TaqMan genotyping master mix, 20ng of genomic DNA and each primer. The PCR conditions were 95°C for 10 min and 40 cycles of 95°C for 15 s and 60°C for 1 min; the resulting products were detected using the ABI PRISM 7900HT Sequence Detection System (Applied Biosystems). Data was analyzed using SDS 2.2 software and CopyCaller software (Applied Biosystems). The *CDKN2A* deletion status shown in Figure 1 was obtained from qPCR results. Only the Hs03714372 assay was used for correlative studies (Figure 2). Only 1 deletion from CGH array analysis did not validate using qPCR (HGG from patient 18) [10].

Fluorescent in Situ Hybridization

Paraffin FISH analysis was performed on four micron tumour sections. Slides were baked

overnight to fix the section to the slide and de-paraffinated using Xylene. Pre-treatment was performed using 10mM Na citrate buffer (pH 6.0) at 80°C for 2 hours, followed by washing in 2X SSC. After 10 minutes in 0.1N HCl for 10 minutes at room temperature, pepsin treatment consisted of 0.1mg (~400U)/mL pepsin in 0.01N HCL at 37°C for 2 to 10 minutes, followed by washing in deionized water, and ethanol dehydration. Slides and probes were co-denatured on the Thermobrite (Intermedico, Markham ON). Denaturation conditions used for paraffin embedded slides/probes were 85°C for 7 minutes, followed by overnight incubation at 37°C. Slides were washed in 0.4x SSC/0.3% NP40 at 73°C for 30 seconds, followed by 2x SSC/0.1% NP40 at room temperature for 30 seconds. Slides were counterstained with DAPI. Hybridized slides were analyzed using a Zeiss Axioplan 2 epifluorescence microscope. Images were captured by an Axiocam MRm Camera (Imaging Associates, Bicester, UK) and analyzed using an imaging system with MetaSystems Isis Software version 5.1.110 (Boston, MA).
FISH was performed using overlapping probes hybridizing to the distal portion of the duplication region (RP11-248P7 and RP11-837G3), labeled in Spectrum green, and control probes in 7p12.1 (RP11-876P22 and RP11-478M17) labeled in Spectrum Orange.

Immunohistochemistry Studies

These studies were performed on 5μm-thick, formalin-fixed, paraffin-embedded tissue sections either as single samples or combined as tissue microarrays containing 1-mm cores derived from the respective tumor blocks. Immunohistochemical studies for the p53 protein were performed using standard techniques as previously reported [11]. P53 dysfunction, characterized by either p53 overexpression and/or *TP53* mutation. Immunohistochemical studies for the *BRAF* V600E mutation were performed using the *BRAF* V600E mutant-specific antibody, VE1 as previously described [12].

C-circle assay to detect ALT phenotype

ALT was detected by screening for c-circles. C-circles are extrachromosomal telomeric repeats (ECTRs) which are ALT specific. They have been found to be robustly associated with ALT and are present in tumors which maintain their telomeres using a recombination phenotype, even following loss of other ALT phenotypic markers[13]. C-circles were detected using a telomere-specific qPCR assay [14].

DNA was diluted to 3.2 ng/μL. 16 ng (5 μL) of DNA was treated with 5 μL of Φ29 master mix containing: 4 mM DTT, 10x Φ29 buffer, 10 μg/μL BSA, 0.1% Tween, 1 mM (each) of dATP, dGTP, dTTP and dCTP, 5 U of Φ29 polymerase.

Following the Φ29 amplification, the samples were diluted to 0.4 ng/μL by adding 30 μL of sterile water to the reaction mixture. Un-treated dilutions of 0.4 ng/μL were also prepared.

The qPCR assay was run with triplicates of Φ29 treated and untreated DNA, requiring a total of 6 PCRs per sample. Each qPCR required 15 μL of master mix and 5 μL (2 ng) of DNA. qPCR master mix contained: 1x QuantiTECT SYBR Green Master Mix (LifeTechnologies - 4309155), 10 mM DTT, 0.5 μL DMSO, and 300 nM of forward primer and 400 nM of reverse primers.

All qPCRs were done in 96 well plates using the Lightcycler 480 (Roche). PCR conditions were: 95 °C for 15 minutes, 35 cycles of 95 °C for 15 seconds (denaturation), and 54 °C for 2 minutes (annealing and elongation). Lightcycler 480 software was used to obtain data.

For determining presence of c-circles, a ΔmeanCp value was calculated for each sample. The ΔmeanCp was the difference between the mean values of the non-Φ29 and Φ29 treated

samples. A positive ΔmeanCp value greater than 0.2 was detected in c-circle positive samples, whereas a negative ΔmeanCp value of less than -0.2 was detected in c-circle negative samples. Samples with ΔmeanCp -0.2 – 0.2 were considered as atypical, and results were confirmed using the dot blot.

Statistical analysis

The Fisher's exact test (correlative studies) and the unpaired two-tailed Student t-test were performed using GraphPad Prism software v6.0 ($P < .05$ was considered significant). Survival analyses were done using the Kaplan-Meier method. Multiple hypothesis testing was accounted for in determining significance. A log-rank test was used to compare groups and curves were generated using Stata v12.

REFERENCES:

1. Torchia EC, Boyd K, Rehg JE, et al: EWS/FLI-1 induces rapid onset of myeloid/erythroid leukemia in mice. Mol Cell Biol 27:7918-34, 2007
2. Cibulskis K, Lawrence MS, Carter SL, et al: Sensitive detection of somatic point mutations in impure and heterogeneous cancer samples. Nat Biotechnol 31:213-9, 2013
3. Wu G, Diaz AK, Paugh BS, et al: The genomic landscape of diffuse intrinsic pontine glioma and pediatric non-brainstem high-grade glioma. Nat Genet 46:444-50, 2014
4. Pfister S, Janzarik WG, Remke M, et al: BRAF gene duplication constitutes a mechanism of MAPK pathway activation in low-grade astrocytomas. J Clin Invest 118:1739-49, 2008
5. Parsons DW, Jones S, Zhang X, et al: An integrated genomic analysis of human glioblastoma multiforme. Science 321:1807-12, 2008
6. Wu G, Broniscer A, McEachron TA, et al: Somatic histone H3 alterations in pediatric diffuse intrinsic pontine gliomas and non-brainstem glioblastomas. Nat Genet 44:251-3, 2012
7. Cheng SP, Hsu YC, Liu CL, et al: Significance of Allelic Percentage of BRAF c.1799T > A (V600E) Mutation in Papillary Thyroid Carcinoma. Ann Surg Oncol, 2014
8. Remke M, Ramaswamy V, Peacock J, et al: TERT promoter mutations are highly recurrent in SHH subgroup medulloblastoma. Acta Neuropathol 126:917-29, 2013
9. Zarghooni M, Bartels U, Lee E, et al: Whole-genome profiling of pediatric diffuse intrinsic pontine gliomas highlights platelet-derived growth factor receptor alpha and poly (ADP-ribose) polymerase as potential therapeutic targets. J Clin Oncol 28:1337-44, 2010
10. Berggren P, Kumar R, Sakano S, et al: Detecting homozygous deletions in the CDKN2A(p16(INK4a))/ARF(p14(ARF)) gene in urinary bladder cancer using real-time quantitative PCR. Clin Cancer Res 9:235-42, 2003
11. Pollack IF, Finkelstein SD, Woods J, et al: Expression of p53 and prognosis in children with malignant gliomas. N Engl J Med 346:420-7, 2002
12. Dahiya S, Haydon DH, Alvarado D, et al: BRAF(V600E) mutation is a negative prognosticator in pediatric ganglioglioma. Acta Neuropathol 125:901-10, 2013
13. Henson JD CY, Huschtscha LI, Chang AC, Au AYM, Pickett HA and Reddel RR: DNA C-circles are specific and quantifiable markers of alternative-lengthening-of-telomeres activity. Nature Biotechnology 27:1181-1186, 2009
14. Lau LMS DR, Henson JD, Au AYM, Royds JA, Reddel RR: Detection of alternative lengthening of telomeres by telomere quantitative PCR. Nucleic Acids Research 41, 2013

Supplementary Figures

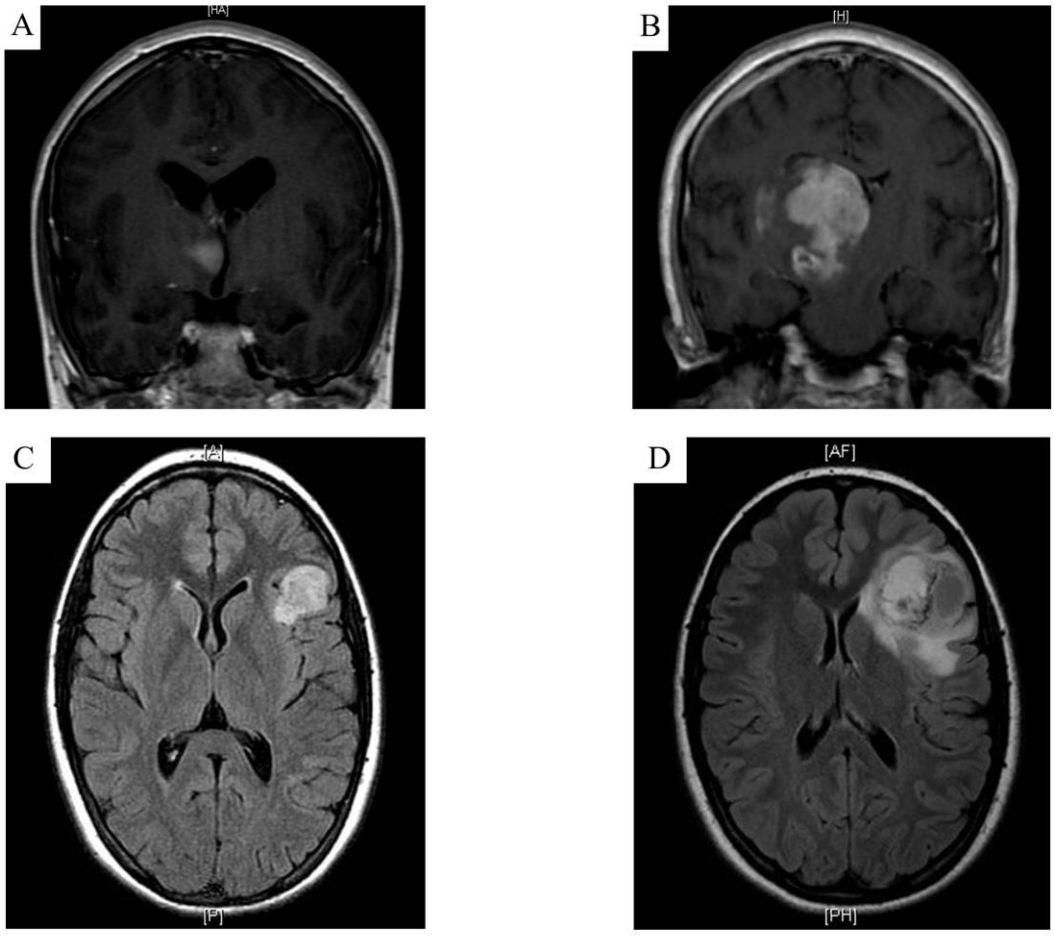

Figure S1: Radiological diagnosis of glioma transformation. Coronal T1 contrast imaging (A) showing small heterogeneously enhancing lesion in the right thalamic region (B) showing heterogeneously enhancing mass with progression, invasion and mass effect indicating sHGG. Low-grade pathological diagnosis was also available. T2 FLAIR axial image for patient 7 shows (C) enhancing lesion in left fronto-temporal cortex (D) Three years after showing heterogeneously enhancing progressive lesion with local invasion and edema with mass effect. Monitoring of the initial low-grade lesion throughout the 3-year latency period was conducted. High-grade pathological diagnosis was also available. Online only.

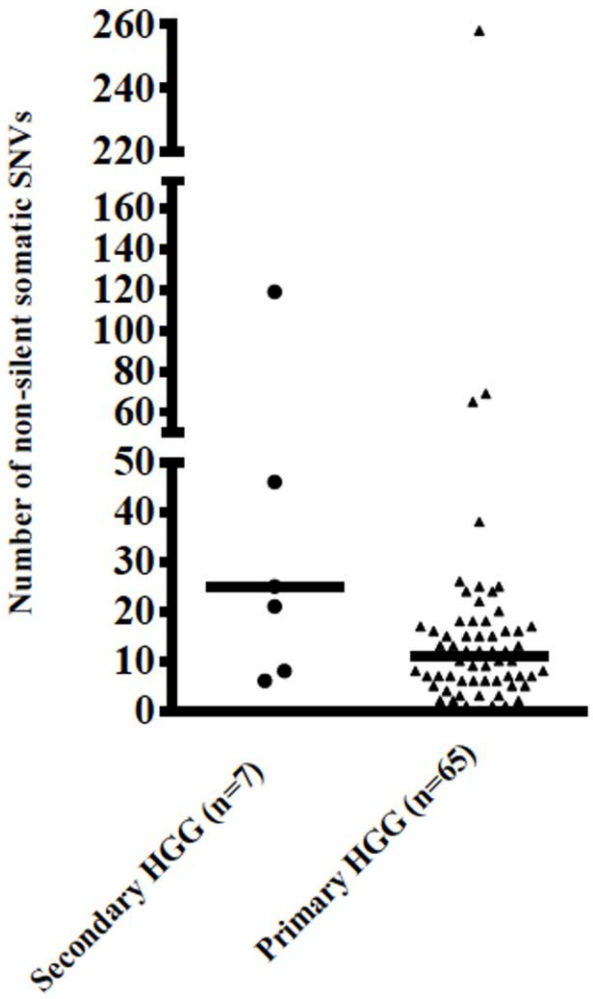

Figure S2: sHGG have a higher non-silent somatic SNV load than primary HGG. Number of non-silent somatic nucleotide variants in 7 secondary (black dots) and 65 primary pediatric HGG (black triangles). Each group had a single HPM tumor (not shown). The median number of mutations in sHGG was 25 versus 11 in primary HGG (P = .0042). Statistical significance was determined using an unpaired two-tailed Student's t-test. Online only.

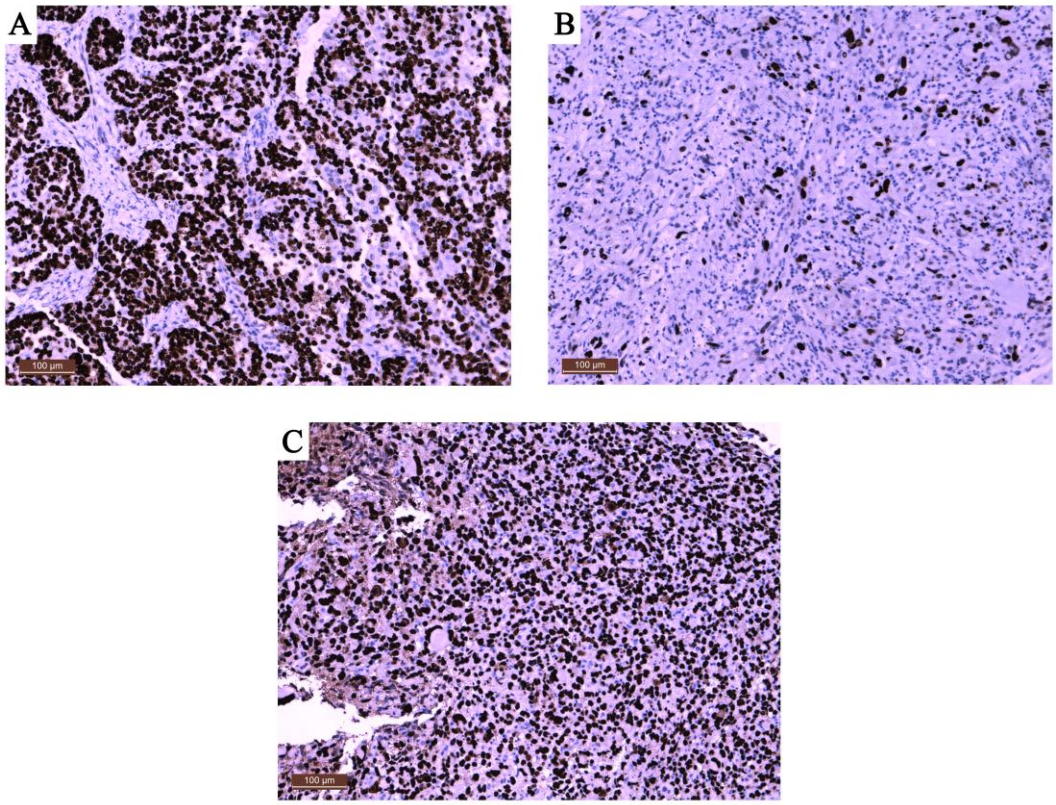

Figure S3: p53 immunoreactivity during malignant transformation in a matched low and high grade tumor pair from patient 16. p53 immunohistochemistry (A) Positive control tissue (B) PLGG with 7% TP53 mutant allelic percentage with weak p53 immunostaining (C) Matching sHGG with 30% mutant allelic percentage with strong p53 staining. Bar represents 100µm length (magnification, x100). Online only.

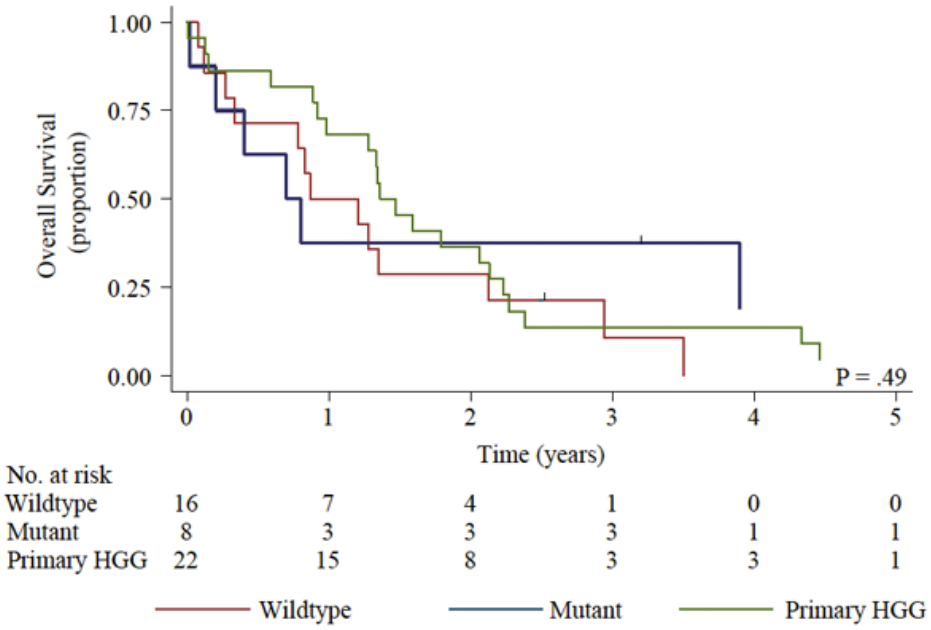

Figure S4: Overall survival estimates following sHGG diagnosis. *BRAF* wildtype sHGG group have a similar overall survival following sHGG diagnosis (3.45% ± 5%), to primary HGG (4.4% ± 4%). The *BRAF* mutant sHGG group showed slightly better overall survival (20% ± 15%), however there was no significant difference in survival between any of these groups (P = .49). Online only.

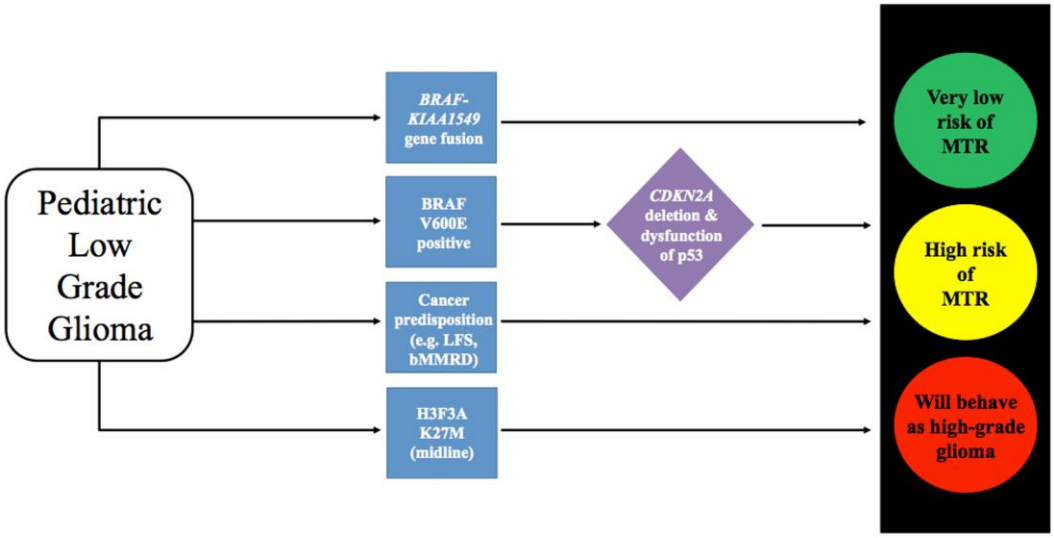

Figure S5: Stratification of PLGG into several risk groups. PLGG harboring the *BRAF-KIAA1549* fusion are at extremely low risk for transformation. BRAF V600E mutant PLGG cases are at high risk of transformation. PLGG from patients with cancer predisposition syndromes will eventually transform to sHGG. Midline PLGG that are H3F3A K27M positive behave as high-grade glioma. Abbreviations: MTR, malignant transformation. Online only.

Patient ID	WHO Grade	Gene	Allele change	Amino acid change	Mutation type	WES	Sanger validated
16	High	*SETD1B*	C>T	R1759C	Missense	Yes	No
19	High	*H3F3A*	A>T	K27M	Missense	No	Yes
7	High	*DOT1L*	C>A	R344S	Missense	Yes	No
20	High	*DNMT1*	C>T	R139K	Missense	Yes	No

Table S2: Somatic point mutations in chromatin-modifier genes of sHGG using WES and Sanger sequencing. Online only.

Patient ID	WHO Grade	Histology	*BRAF* V600E - WES	*BRAF* V600E - Sanger	*BRAF* V600E - castPCR	*BRAF* V600E - IHC
1	Low	PA	N/A	N/A	0%	N/A
2	Low	PA	N/A	WT	N/A	N/A
3	Low	LGA	N/A	WT	N/A	N/A
4	Low	LGA	N/A	N/A	0%	N/A
	High	GBM	N/A	N/A	0%	N/A
5	High	AA	N/A	N/A	N/A	WT
6	High	GBM	N/A	WT	N/A	N/A
7	High	AA	WT	WT	0%	N/A
8	High	AA	WT	WT	0%	N/A
9	High	APXA	WT	WT	0%	N/A
10	Low	PXA	N/A	WT	0%	N/A
	High	APXA	N/A	WT	0%	N/A
11	Low	PA	N/A	WT	N/A	N/A
12	Low	LGA	N/A	WT	0%	N/A
13	Low	PA	N/A	WT	0%	N/A
	High	AA	N/A	WT	0%	N/A
14	Low	PA	N/A	WT	0%	N/A
	High	GBM	N/A	WT	N/A	N/A
15	Low	PXA	N/A	WT	0%	N/A
16	Low	PXA	HET	HET	9.09%	N/A
	High	APXA	WT	WT	0%	N/A
17	Low	PXA	N/A	HET	47.10%	N/A
18	High	GBM	HET	HET	16.30%	N/A
19	Low	GG	HET	HET	28.90%	N/A
	High	AGG	HET	HET	5.05%	N/A
20	Low	LGA	N/A	HET	26.90%	N/A
	High	GBM	HET	HET	35.70%	N/A
21	Low	PXA	N/A	HET	21.20%	N/A
	High	GBM	N/A	HET	77.20%	N/A
22	Low	GG	N/A	HET	N/A	N/A
	High	AGG	N/A	HET	N/A	N/A
23	Low	LGA	N/A	HET	N/A	N/A
	High	GBM	N/A	HET	N/A	N/A
24	Low	LGA	N/A	HET	56.70%	N/A
	High	GBM	N/A	N/A	N/A	HET

Table S3: BRAF V600E genotyping from whole-exome and Sanger sequencing, castPCR and immunohistochemistry. Abbreviations: N/A, not applicable. Online only.

Pathology types	N	%
Pilocytic astrocytoma	72	43.1
Low-grade astrocytoma - NOS	57	34.1
Ganglioglioma	23	13.8
Pleomorphic xanthoastrocytoma	5	3.0
Pilomyxoid astrocytoma	6	3.6
Mixed/Oligoastrocytoma	4	2.40
Total	167	100

Table S4: PLGG used for BRAF mutation correlative studies

Patient ID	Grade	Histology	9p21.3 deletion array-CGH	Chr.9:21994261 on NCBI build 37 (*CDKN2A*)	Chr.9:21967916 on NCBI build 37 (*CDKN2A*)
2	High	GBM	N/A	N/A	Balanced
4	Low	LGA	N/A	N/A	Balanced
6	High	GBM	N/A	N/A	Balanced
7	High	AA	Balanced	Balanced	Balanced
8	High	AA	Homozygous deletion	Homozygous deletion	Homozygous deletion
9	High	APXA	Homozygous deletion	N/A	Homozygous deletion
10	High	APXA	N/A	Hemizygous deletion	Hemizygous deletion
11	Low	PA	N/A	N/A	Balanced
12	Low	LGA	N/A	N/A	Hemizygous deletion
13	Low	LGA	N/A	N/A	Hemizygous deletion
14	Low	LGA	N/A	N/A	Hemizygous deletion
	High	GBM	N/A	N/A	Homozygous deletion
15	Low	PXA	N/A	N/A	Hemizygous deletion
16	Low	PXA	Homozygous deletion	Homozygous deletion	Homozygous deletion
	High	APXA	Balanced	Balanced	Balanced
17	Low	PXA	N/A	Homozygous deletion	Homozygous deletion
18	High	GBM	Hemizygous deletion	Balanced	Balanced
19	Low	GG	Balanced	Balanced	Balanced
	High	AGG	Balanced	Balanced	Balanced
20	Low	LGA	N/A	N/A	Balanced
	High	GBM	Hemizygous deletion	Hemizygous deletion	Hemizygous deletion
21	Low	PXA	N/A	N/A	Homozygous deletion
	High	GBM	N/A	N/A	Homozygous deletion
22	Low	GG	N/A	N/A	Hemizygous deletion
	High	AGG	N/A	N/A	Hemizygous deletion
23	Low	LGA	N/A	N/A	Homozygous deletion
	High	GBM	N/A	N/A	Homozygous deletion
24	Low	LGA	N/A	Homozygous deletion	Homozygous deletion

Table S5: Heterozygous and homozygous deletions of 9p21.3 (*CDKN2A*) using array-CGH and real-time qPCR. Online only.

Pathology type	N	%	% transformation
Pilocytic astrocytoma	288	40.6	2.4
Low-grade astrocytoma - NOS	252	35.5	3.6
Ganglioglioma	66	9.3	3.0
Pleomorphic xanthoastrocytoma	10	1.4	50.0
Pilomyxoid astrocytoma	10	1.4	0
Mixed/Oligodendroglioma	42	5.9	0
SEGA	23	3.2	0
Others	19	2.7	0
Total	710	100	
PLGG without pathological diagnosis			
Optic pathway glioma (NF1)	143 (111)	81.3	0
Brainstem	11	6.2	18
Tectal	22	12.5	0
Total	176	100	
Final total	886		

Table S7: Pediatric low grade gliomas treated at the Hospital for Sick Children during study period. Others: Astroblastoma, angiocentric glioma, fibrillary astrocytoma, dysembryoplastic neuroepithelial tumors. Out of 886 total patients in The Hospital for Sick Children database, initial pathological diagnosis was available for 710 (80.1%) patients. One hundred and seventy six (19.9%) patients did not have low grade pathological diagnosis and were followed on the basis of clinic-radiological diagnosis. Most of these patients had either optic pathway glioma (81.3%, out of which 78% were patients diagnosed with NF1) or tectal tumors. Abbreviations: NOS, not otherwise specified; SEGA, subependymal giant cell astrocytoma; NF1, Neurofibromatosis type I; Mixed, mixed glioma.